Isı Bilimi ve Tekniği Dergisi, 40, 2, 367-378, 2020
J. of Thermal Science and Technology

ISSN 1300-3615
https://doi.org/10.47480/isibted.817194

ELECTRICAL AND THERMAL CONDUCTIVITY AND PHONON CONTRIBUTION TO THE THERMAL CONDUCTIVITY IN THE BI-IN SYSTEM

Pınar ATA ESENER*, Ümit BAYRAM, Esra ÖZTÜRK***, Sezen AKSÖZ**** and Necmettin MARAŞLI*****

* Erciyes University, Institute of Natural and Applied Sciences, Kayseri, 38039, Turkey, pinarata_88@hotmail.com, ORCID: 0000-0002-6498-4534

** Erciyes University, Institute of Science and Technology, ERNAM-Nanotechnology Research and Application Center, Kayseri 38039, Turkey, umitbayram14@gmail.com, ORCID: 0000-0001-8760-8024

*** Kocaeli University, Department of Physics, Kocaeli, 41380, Turkey, esra3.ozturk@gmail.com, ORCID: 0000-0002-3531-7564

**** Nevşehir Hacı Bektaş Veli University, Department of Physics, Nevşehir, 50300, Turkey, sezenaksoz@nevsehir.edu.tr, ORCID: 0000-0002-8990-1926

***** Yıldız Technical University, Department of Metallurgical and Materials Engineering, İstanbul, 34210, Turkey, nmarasli@yildiz.edu.tr, ORCID: 0000-0002-1993-2655

(Geliş Tarihi: 07.07.2020, Kabul Tarihi: 20.10.2020)

Abstract: In this study, the contribution of phonon to the thermal conductivity in the In-Bi (Indium-Bismuth) system due to its composition variation was determined from their electrical and thermal conductivity measurements. Because of the common usage of In-Bi system in many technological applications, thermal and electrical conductivity variations with temperature for different compositions of Bi component were measured. Four-Point Probe (FPP) and Linear Heat-Flow (LHF) methods were used for electrical and thermal conductivity measurements respectively. Intermetallic systems' electrical conductivity values were determined between 0.8524 (1/Ω m) $\times 10^6$ and 2.8381(1/Ω m) $\times 10^6$ and thermal conductivity values were found between 14.50 (W/Km) and 35.93 (W/Km) at the melting temperature. Electron and phonon contributions to the thermal conductivity were calculated by using Wiedemann-Franz Law (WFL) from the measured values. The temperature coefficients values (α) of electrical and thermal conductivity were calculated between 0.46-2.54 (K^{-1}) $x10^{-3}$ and 1.29-4.34 (K^{-1}) $x10^{-3}$ respectively. In order to observe microstructure of the Bi-In intermetallic alloy Scanning Electron Microscopy (SEM) and to determine the composition of the phases in the structures, Energy Dispersive X-Ray Analysis (EDX) were used. Also melting temperatures (349.03 K-387.24 K), enthalpy of fusion (17.97 J/g- 42.37 J/g) and specific heat change (0.159 J/gK-0.372 J/gK) of Bi-In alloy systems were measured by using Differential Scanning Calorimeter (DSC).
Keywords: Microstructure, Electrical properties, Thermal properties.

BI-IN SİSTEMİNDE ELEKTRİKSEL VE ISIL İLETKENLİK VE ISIL İLETKENLİĞE FONON KATKISI

Özet: Bu çalışmada, elektriksel ve ısıl iletkenlik ölçümleri kullanılarak ısısal iletkenliğe fonon katkısı kompozisyon değişimine bağlı olarak belirlenmiştir. In-Bi sistemlerinin birçok teknolojik uygulamalarda yaygın olarak kullanılması sebebiyle farklı kompozisyonlardaki Bi bileşimlerinin sıcaklığa bağlı elektriksel ve ısıl iletkenlik değişimleri ölçülmüştür. Elektriksel ve ısıl iletkenlik ölçümlerinde sırasıyla Dört Nokta Prob (FPP) ve Lineer Isı Akışı (LHF) yöntemleri kullanılmıştır. Erime sıcaklığında, intermetalik sistemlerin elektriksel iletkenlik değerleri 0.8524 (1/Ω m) $\times 10^6$ ve 2.8381(1/Ω m) $\times 10^6$ arasında ve ısısal iletkenlik değerleri 14.50 (W/Km) ve 35.93 (W/Km) arasında bulunmuştur. Ölçülen değerlerle, Wiedemann-Franz Kanunu (WFL) kullanılarak, ısıl iletkenliğe elektron ve fonon katkısı hesaplanmıştır. İntermetalik alaşım sistemleri için, elektriksel ve ısıl değerlerin sıcaklık katsayıları (α) sırasıyla 0.46-2.54(K^{-1}) $x10^{-3}$ ve 1.29-4.34 (K^{-1})$x10^{-3}$ aralığında hesaplanmıştır. Bi-In İntermetalik alaşım sistemlerinin mikroyapılarını gözlemlemek için Taramalı Elektron Mikroskobu (SEM) ve yapılardaki fazların kompozisyonlarını belirlemek için, Enerji Dağıtıcı X-Işını (EDX) analizi kullanılmıştır. Bi-In alaşım sistemlerindeki erime sıcaklıkları (349.03 K-387.24 K), füzyon entalpisi (17.97 J/g- 42.37 J/g) ve spesifik ısı değişimi (0.159 J/gK-0.372 J/gK) Diferansiyel Taramalı Kalorimetre (DSC) ile ölçülmüştür.
Anahtar Kelimler: Mikroyapı, Elektriksel özellikler, Isıl özellikler.

NOMENCLATURE

In	Indium
Bi	Bismuth
Zn	Zinc
Ag	Silver
Sb	Antimony
Sn	Tin
wt.	Weight
mm	Milimeter
mL	Mililiter
g	Gram
FPP	Four-point probe
LHF	Linear heat flow
WFL	Wiedeman Franz law
SEM	Scanning electron microscopy
EDX	Energy dispersive X-ray
DSC	Differential scanning calorimeter
$K_{thermal}$	Total thermal conductivity
K_e	Electron contribution to the thermal conductivity
K_{ph}	Phonon contribution to the thermal conductivity
σ	Electrical conductivity
α_{ETC}	Eectrical conductivity's temperature coefficient
T_0	Set reference temperature
α_0	Electrical conductivity at Temperature T_0
RCF	Resistivity correction factor
V	Voltage
I	Current
A	Amper
K	Kelvin
G	Coefficient that includes the surface geometric boundaries and thickness of the sample.
s	The difference between probes,
t	The thickness of the sample
d	The diameter of the sample.
Q	Input power
A	Cross-sectional area of the specimen
ΔT	Temperature difference
ΔX	Distance between two measurement points
H	Enthalpy
ΔC_P	The change of specific heat
T_M	The melting temperature
T_{max}	Peak temperature
T_{end}	End temperature
T_{onset}	Onset temperature

INTRODUCTION

Electrical and thermal conductivity values are very crucial parameters for intermetallic and metallic alloy systems owing to their wide variety of the use in practical application in industry and electronics. In reported works, there is no detailed investigation and explanation about thermal and electrical conductivities of intermetallic alloy systems. Therefore, providing thermal and electrical conductivity values for intermetallic alloy systems will be beneficial for researchers. In this work, seven different intermetallic compositions of Bi-In system were chosen to measure the electrical and thermal conductivities.

The thermal conductivity of a material can be defined as the rate of heat transfer through an unit thickness of the material per unit area per unit temperature difference. In solids, heat conduction depends on two effects: the lattice vibrational waves induced by the vibrational motions of the molecules positioned at relatively fixed positions in a periodic manner called lattice, and the energy transported via free flow of electrons in solid. The thermal conductivity of a solid is obtained by adding the lattice and electronic components. Thus, the total value of thermal conductivity (K) can be identified with the equation below.

$$K_{thermal} = \frac{1}{3} \sum_j C_j \, v_j \, l_j \qquad (1)$$

Here j shows sort of the carrier, C_j means specific heat per unit volume, v_j is the velocity of the carrier and l_j is mean free path.

In a metal, major heat carriers are electrons and phonons. The total thermal conductivity can be written as the sum of both electron and phonon contributions as shown below;

$$K_{thermal} = K_e + K_{ph} \qquad (2)$$

here K_e is the electron contribution and K_{ph} is the phonon contribution (Touloukian et al., 1970). In pure metals, the electrons' contribution is bigger than the phonons'. However, in impure metals they are nearly same (Kittel, 1965).

The value K_e can be calculated by using the Wiedeman Franz Law (WFL) (Kittel, 1965) as shown in Eq. (3). Here σ is the electrical conductivity value, L is Lorentz number that equals to $2.44 \times 10^{-8} W\Omega K^{-2}$ (Kittel, 1965) and T is the given temperature value.

$$\frac{K_e}{\sigma} = LT \qquad (3)$$

The main idea behind of this research was to calculate the phonon contribution in binary alloys. In order to determine this contribution, we measured the variation of the electrical and thermal conductivity with respect to different temperatures by using Four-Point Probe (FPP) and Linear Heat Flow (LHF) methods. The electron contribution to thermal conductivity (K_e) was calculated from WFL at given temperature by the help of calculated electrical conductivity (σ) values. Then the phonon contribution (K_{ph}) was calculated by Eq. (2) providing K_e and $K_{thermal}$ values which were obtained before.

In the present work, Bi-12 wt.% In, Bi-15 wt.% In, Bi-35.4 wt.% In, Bi-45 wt.% In, Bi-47.6 wt.% In, Bi-53 wt.% In, Bi-62 wt.% In binary alloys' thermal and electrical conductivity values were measured.

It is difficult to produce wires or sheets by using Bi-based alloys because of bismuth's brittle nature and its tendency to segregation. Therefore, Bi-based alloys are inappropriate for many technological applications. Although some particular compositions of Bi-In binary alloys are used for lead-free solders owing to their low-melting point (Sun et al., 2014; Takahashi et al., 1977; Sammes et al., 1999; Jiang et al., 2002). Bi-In based ternary alloys including Zn, Ag, Sb and Sn are mostly used as lead-free solders in electronical industry. Bi-In-Sn is the most promising one within these ternary alloy systems. The mechanical properties improve significantly by adding Sn into the Bi-In binary alloy. At the previous studies (Pandher and Healey, 2018; Pandher et al., 2007; Huang and Wang et al., 2005; Liu and Shang, 2001; Zhao et al., 2004; Cheng at al. 2017), it has been found that adding Bi to lead-free solders has healing properties in alloys such as wettability, solder spreading, and reducing melting temperature and Bi can reduce the surface tension of the alloy compared to Sn. However, there are several binary and eutectic compounds that have low melting points as a result of melting in the Bi-In system. At a relatively high operating temperature of some soldering interconnects, serious problems arise regarding the effect of reaction products at the solder/substrate interface on the performance and reliability of the connections. Even small changes in the chemical composition of the interface between solder alloy and substrate, can lead to large changes in macroscopic behavior of soldered zone. Hence this effects the reaction behavior and morphological evolution of the solder-substrate system and therefore further progress in these areas become difficult (Biglari et al., 2018). In addition to use of Bi-In intermetallic compounds containing Zn in the production of alkaline batteries, Bi-In amalgams have been used to improve the properties of the fluorescent lamps. Thus, the knowledge of thermophysical properties of the Bi-In based ternary alloys, which have many technological applications, are very crucial (Sun et al., 2014; Takahashi et al., 1977; Sammes et al., 1999; Jiang et al., 2002; Rudnev et al., 2003; Yang et al., 2011; Liu et al., 2010; Bencze, 2006; Vizdal et al., 2007; Yang and Messler, 1994). In this study, in order to contribute to the thermophysical properties of Bi-In based ternary alloys, electrical and thermal conductivities of seven different intermetallic phases of Bi-In binary alloy have been investigated. These intermetallic phases of the Bi-In binary alloy system are Bi_4In, Bi_3In, BiIn, Bi_2In_3, Bi_3In_5, $BiIn_2$ and $BiIn_3$ (ASM, 1992). In order to obtain these metallic phases, the compositions of Bi-In binary alloys were chosen as Bi-12 wt.% In, Bi-15 wt.% In, Bi-35.4 wt.% In, Bi-45 wt.% In, Bi-47.6 wt.% In, Bi-53 wt.% In, Bi-62 wt.% In by the help of phase diagram in previously published work (ASM, 1992).

In this study, the first step was to measure electrical and thermal conductivity variations with temperature. The second step was to obtain the phonon contribution to thermal conductivity. Finally, the microstructure and structural characteristics of Bi-In intermetallic alloys were investigated by using Scanning Electron Microscopy (SEM), Energy Dispersive X-Ray Analysis (EDX) and Differential Scanning Calorimeter (DSC).

EXPERIMENTAL PROCESS

Production of the samples

Bi-12 wt.% In, Bi-15 wt.% In, Bi-35.4 wt.% In, Bi-45 wt.% In, Bi-47.6 wt.% In, Bi-53 wt.% In and Bi-62 wt.% In alloys were prepared in a vacuum furnace system. Graphite crucibles that used in production, are drilled with 50 mm depth and 8 mm diameter for thermal conductivity measurements. During the experimental process, an alumina tube was used to facilitate the insertion of the thermocouples that used to determine the temperature difference into the sample. For this reason, 1.2 mm diameter hole was drilled at the rear end of the sample crucible. The sample crucibles that used for electrical conductivity measurements were also processed on a lathe to be 50 mm depth and 4 mm in diameter. Two different castings were made for both electrical and thermal conductivity measurements. Metals with 99.9% purity were melted in a vacuum melting furnace. The melted metals were stirred at regular intervals to form an alloy. The molten alloy was placed in a heated casting furnace for unidirectional solidification and left to solidify for one day. Also the same process was repeated for the production of the other alloy systems. The produced alloys have been prepared for the measurements and analyzes by cutting them in appropriate sizes according to their usage areas like thermal and electrical conductivity, microstructure and thermal properties. The samples used for conductivity measurements were prepared under directionally solidification. The details of the experimental system can be found in Refs Gündüz and Hunt (1985), Maraşlı and Hunt (1996), Aksöz (2013).

Microstructure of the Systems

In order to observe microstructure and determination of the phases in the sample, SEM was used for different compositions of the In-Bi alloy system. Well-known metallographic process as polishing and etching were used to pick out the different phases in the microstructure. Bi-12 wt.% In, Bi-15 wt.% In, Bi-35.4 wt.% In were etched for 5-10 seconds in the mixture of 20 mL hydrogen chloride, 4 g picric acid and 400 mL of ethanol. Bi-45 wt.% In, Bi-47.6 wt.% In, Bi-53 wt.% In, Bi-62 wt.% In were etched for 5-10 seconds in proper solution prepared with 1.3 g of potassium dichromate,

4.3 mL of sulfuric acid, 2.7 mL of sodium chloride, 17.7 mL of hydrogen fluoride, 8.8 mL of nitric acid and 66.3 mL of water. SEM images of the microstructures and EDX analysis of the In-Bi alloy samples with different composition were carried out to obtain the phases of Bi-In intermetallic alloys. As an example, in Figure 1, SEM image and EDX analysis results are given together for Bi-12wt. %In system.

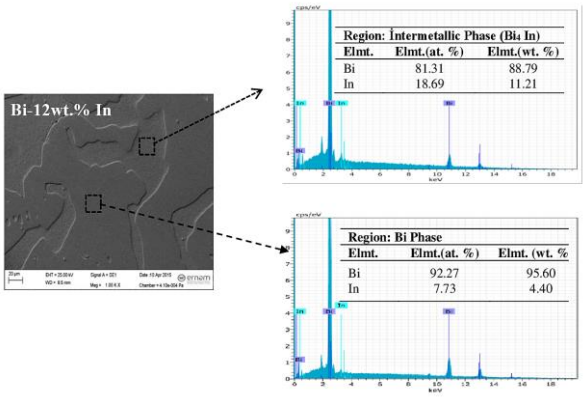

Figure 1. The chemical composition analysis of Bi-12 wt.% In alloy by using EDX.

Electrical Conductivity

Electrical conductivity is an essential characteristic for metallic alloy systems and affected by many parameters such as impurities, heating process, grain size and plastic deformation. However, the temperature and the chemical composition affect the electrical conductivity more than other parameters (Rudnev et al., 2003).

The vibration of the atoms increases with the increasing of the temperature and these vibrations result in some dislocations (Meydaneri et al., 2012). Probability of the electron waves deviation increases owing to the dislocations that are formed in the corners of the blank lattice, grain boundaries, and via substituted atoms (Onaran, 2009). These dislocations result in increasing inelastic collisions between electrons-phonons and mean free path decreases with increasing collisions. So, electrical resistivity of the metal increases and electrical conductivity decreases by the rise in temperature. The dependency of electrical conductivity to the temperature is shown in Eq. (4)

$$\sigma(T) = \sigma_0\left[1 + \alpha_{ETC}(T - T_0)\right] \quad (4)$$

where, α_{ETC} is electrical conductivity's temperature coefficient, T_0 is the set reference temperature (generally room temperature), σ_0 is the conductivity at temperature T_0. α value can be expressed as;

$$\alpha_{ETC} = \frac{\sigma - \sigma_0}{\sigma_0(T - T_0)} = \frac{1}{\sigma_0}\frac{\Delta\sigma}{\Delta T} \quad (5)$$

The resistivity of a sample in FPP system as shown in Figure 2 can be written as

$$\rho = RCF\frac{V_{measured}}{I_{measured}} \quad (6)$$

here RCF called resistivity correction factor which is obtained from thickness, the size of structure, electrode and the position of electrodes (Valder, 1954). Electrical resistivity is calculated by measuring the current and voltage values of four probes that positioned with a distance of 1 mm. Two inner probes measure voltage (V) and outer two probes measure current (I) values.

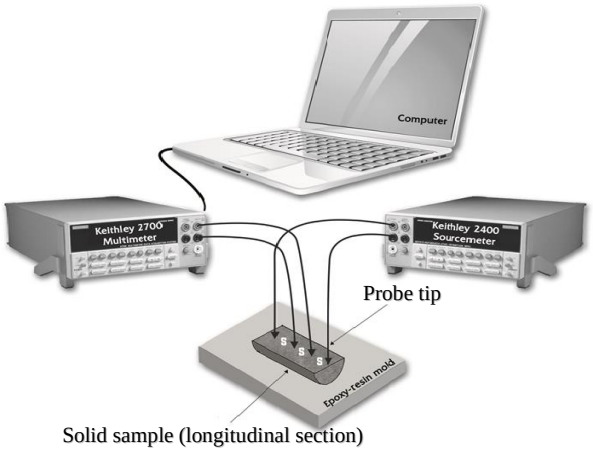

Figure 2. The schematic diagram of four-point probe method used for measuring electrical resistivity/conductivity.

The geometric properties of the materials are also important for determining the electrical resistivity values of the materials. The electrical resistivity expression is given as;

$$\rho = \frac{V_{23}}{I_{14}}G \quad (7)$$

where G is a coefficient that includes the surface geometric boundaries and thickness of the sample. The geometry of the samples are discs with a thickness t and a circle geometry of diameter d. The dimensions of these discs and the distance s between the terminals are measured. Also the ratios of geometry are calculated. Looking at these rates, it is seen that s≥1 and d / s <40. In this case, the required geometric correction factor is calculated by the following equation.

$$G = 2\pi s F_1(t/s)F_2(d/s) \quad (8)$$

where s is the difference between probes, t is the thickness and d is the diameter of the sample. F_1 and F_2 are correction functions (Yılmaz, 2008). In order to determine the electrical resistivity value, the cast alloys are cut in 35 mm length in the precision cutting device and made ready to be placed in the FFP system. FPP

system consists of Keithley 2400 programmable power supply, Keithley 2700 multimeter, Proterm ash furnace and a computer. For each sample the electrical resistivity values were calculated by writing the current and voltage values that measured from the FPP system into Eq. (7). Electrical resistivity values were determined with approximately 5 % error.

Thermal Conductivity

In this study, a LHF apparatus which can reach up to 673 K and can be set to the desired temperature has been used to measure the thermal conductivity of solids. The system has three parts called hot-stage, cold-stage and sample holder as shown in Figure 3. The specimen is heated from one side by using the hot stage in steps of 20 K up to approximate 10 K below the melting temperatures of the materials and the other side of the specimen was kept cool by using a cold stage to get linear temperature gradient. The hot-stage is composed of two brass plates, which are heated by NiCr wires. A transformer was placed in the supply circuit to maximize the thermal stability of the hot-stage, stepping the maximum current down to 4 A. The temperature of the hot-stage was controlled with an accuracy of ±0.01 K with a Eurotherm 2604 type controller. The cold-stage's design is similar with the hot-stage. However, cooling is accomplished by using a Poly Science digital 9102 model heating/refrigerating circulating bath that contains an aqueous ethylene glycol solution.

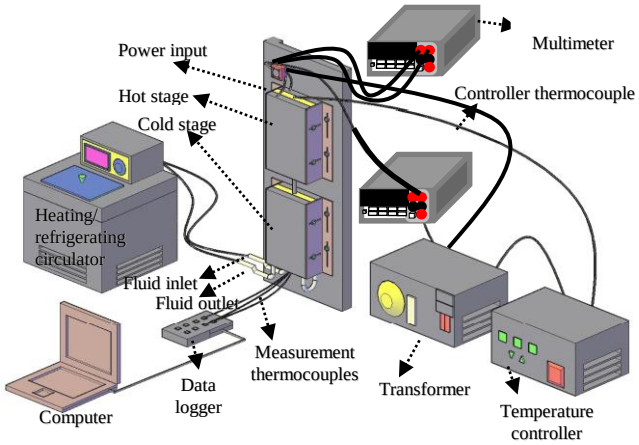

Figure 3. Block diagram of linear heat flow apparatus used for measuring thermal conductivity.

The baths temperature were kept constant at 278 K with an accuracy of ± 0.01 K. The distance between the hot stage and cold stage was kept by 10 mm to get a linear temperature gradient into specimen. Sample holder consists of two copper plates. To place the specimen between the hot and cold stages and get good heat conduction trough to specimen, two holes were drilled at cross sections of cold and hot copper plates. At the same time, a hole was also drilled to insert the measurement thermocouples into specimen. The ends of specimen were tightly fitted into holes at cold and hot copper plates. Thermocouples were then placed into specimen by inserting thermocouples through the hole of cold plate. Then, top and bottom copper plates include the specimen were placed together into hot and cold stages (Gündüz and Hunt,1985; Maraşlı and Hunt, 1996; Valder, 1954; Ocak et al., 2008; Ata Esener et al., 2019; Akbulut et al., 2008; Akbulut et al., 2009; Keşlioğlu et al., 2006; Karadağ et al., 2018; Altıntas et al., 2016; Pietenpol and Miley, 1929).

The thermal conductivity (K) at steady-state condition could be determined by the one-dimensional Fourier-Biot equation, (Kittel, 1965; Touloukian et al., 1970)

$$K = -\frac{Q\,\Delta X}{A\,\Delta T} \tag{9}$$

here Q is the input power and A is the cross-sectional area of the specimen. $\Delta T = T_2 - T_1$ is the temperature difference and $\Delta X = X_2 - X_1$ is the distance between two measurement points.

To have a constant linear temperature gradient at the LHF system, while one side of the specimen was heated with a hot stage and the other side of specimen was cooled by the help of cold stage. The specimen has been kept for at least two hours to reach equilibrium at each measurement temperature.

One has to measure Q, A, ΔT and ΔX, to evaluate the thermal conductivity of a binary alloy system from Eq. (9). Q was determined for every measurement temperature by measuring the input power given into the linear heat flow system for without (Q_{WOS}) and with specimen (Q_{WS}). The cross-sectional area of the specimen ($A = \pi r^2$) was calculated by measuring the radius of the specimen. The temperature difference (ΔT) between two thermocouples was determined via a data-logger. The distance between two measurement points (ΔX) was determined from the photos of the thermocouple's positions. After the measurement of A, $Q = Q_{WS} - Q_{WOS}$, ΔT and ΔX values, the thermal conductivities of Bi-In intermetallic alloy systems were determined from Eq. (9).

For solid phase, the temperature dependency of the thermal conductivity is given as (Touloukian, 1970; Callendar and Nicolson, 1897)

$$K_S = K_{S0}\left[1 + \alpha_{TTC}\left(T - T_0\right)\right] \tag{10}$$

here K_S and K_{S0} are thermal conductivity values of the solid phase at temperature T and reference temperature T_0, respectively and α_{TTC} is thermal temperature coefficient. By using Eq. (10),

$$\alpha TTC = \frac{Ks - Ks0}{Ks0\left(T - T0\right)} = \frac{1}{Ks0}\frac{\Delta K}{\Delta T} \tag{11}$$

can be written. The $\frac{\Delta K}{\Delta T}$ expression is the slope of the graph of thermal conductivity with temperature. So α_{TTC} can be determined by Eq. (11) with the help of this graph.

Experimental error in measuring thermal conductivity is equal to the sum of the uncertainties in the measurements of the heat flow rate, the temperature difference, the cross sectional area of the sample and the thermocouple locations. The total uncertainty in the measurements of thermal conductivity in this study is approximately 9%, since there is an error of around 5% from the heat flow rate, around 2.5% from the measurement of temperature differences, around 0.5% from the measurement of the cross-sectional area and around 0.3% from the fixed distance measurement.

The Enthalpy of Fusion and the Specific Heat Change of the Materials

The specific heat of a material (at a constant pressure) is given as

$$C_p = \left(\frac{\partial H}{\partial T}\right)_p \quad (12)$$

By integration of Eq. (12), the enthalpy of a material, can be obtained as (H=0 at 298 K)

$$H = \int_{298}^{T} C_p dT \quad (13)$$

During the phase transformation from solid to liquid phase with given heat, the temperature of the sample doesn't increase. This heat has been called enthalpy of fusion or latent heat of melting and used to transform from solid to liquid phase. The enthalpy of fusion can be given as

$$\Delta H \approx \Delta C_p T_M \quad (14)$$

here ΔC_P is the change of specific heat and T_M is the melting temperature. Since the enthalpy of fusion and the specific heat of Bi-In alloys are necessary for practical application in industry, these parameters have been measured in present work. Bi-In intermetallic alloys have been heated by using a *Perkin Elmer Diamond* model DSC with a heating rate of 10 K/min up to 823 K. The variations of heat flow with temperature for Bi-In intermetallic alloys.

RESULTS AND DISCUSSION

Microstructure

Different amounts of In were added to the Bi-[*x*] wt.% In systems in order to improve the properties of them. The amounts of In in the Bi-[*x*] wt.% In system were chosen from the phase diagram (ASM, 1992) as 12, 15, 35.4, 45, 47.6, 53 and 62 wt.%, respectively. By scanning every region of the used phase diagram (ASM, 1992), changes in the microstructure were observed with the dependence of In amount.

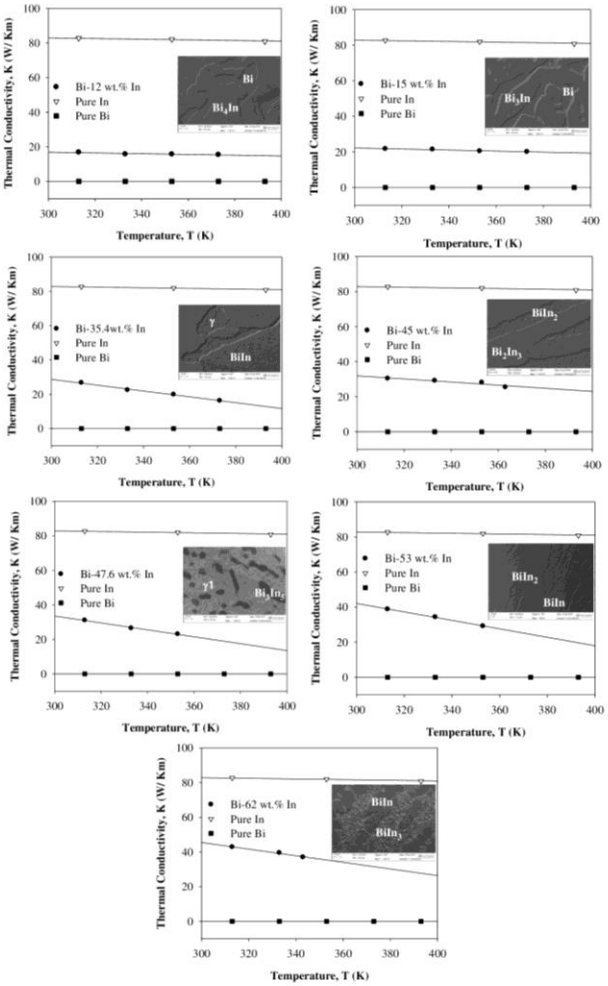

Figure 4. The thermal conductivity variations with temperature and microstructure images for Bi-In intermetallic alloys.

As can be seen in SEM images of Bi-53wt.% In and Bi-62wt.% In alloys, as the amount of In in alloys increases, the intermetallic BiIn is less observed. The pattern for Bi-45 wt.% In alloy indicate two phases, Bi_2In_3 intermetallic phase and a secondary phase of $BiIn_2$ intermetallic phase. The matrix phase with the dark grey colour is Bi_2In_3, the dark needle like and platelet phase is the $BiIn_2$ intermetallic phase as shown for Bi-62wt.% In alloy, too. Bi-47.6 wt.% In alloy show simple structure that Bi_3In_5 phase is homogenously dispersed in the Bi-rich phase γ. Bi-62 wt.% In has fewer of the BiIn intermetallic phase than Bi-35.4 wt.% In alloy. But it has different intermetallic phase which the white platelet is the $BiIn_3$. EDX results show that Bi, γ (Bi Rich), Bi_4In, Bi_3In, BiIn, Bi_2In_3, Bi_3In_5, $BiIn_2$ and $BiIn_3$ phases were determined respectively in compatible with the phases on the phase diagram (ASM, 1992).

The Enthalpy of Fusion and the Specific Heat Change of Material

The variations of heat flow with temperature for Bi-In alloys have measured by DSC equipment and the graphs have been given in Figure 5.

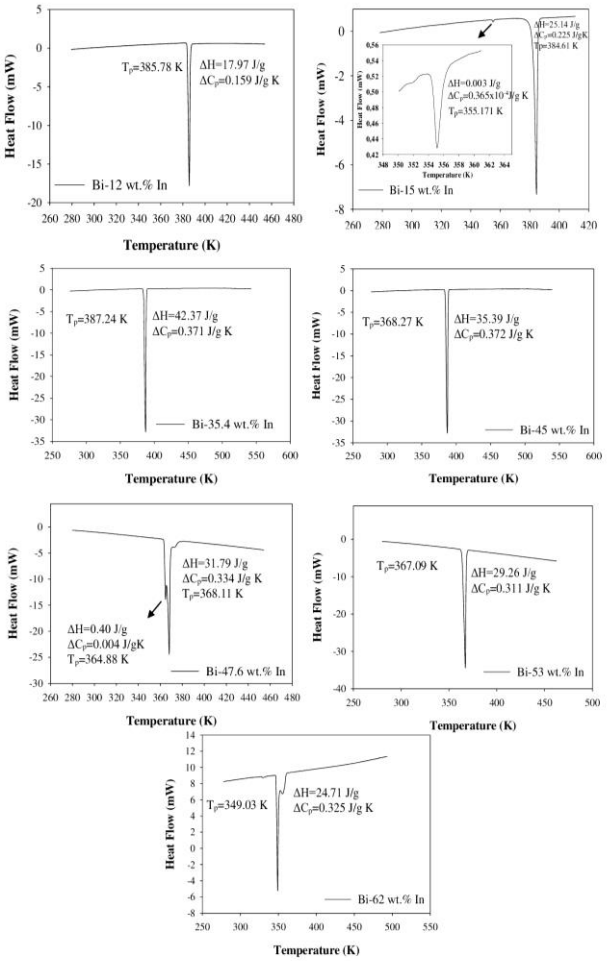

Figure 5. The heat flow versus temperature curve for Bi-In intermetallic alloys at heating rate of 10 K/min.

Onset, maximum and end peak temperatures, the pasty range temperature, enthalpy and specific heat for melting progress were calculated from the Figure 5 and given in Table 1. Melting points of the Bi-[*x*] wt.% In (*x*=12, 15, 35.4, 45, 47.6, 53 and 62) alloys decreases with of In concentration, and the pasty ranges of the alloys are enlarged simultaneously.

As seen from Table 1, the increment in transition temperature range is considered as a disadvantage. Because when phase transition temperature range is increased, the soldering wire may be solidified later than expected. However, at this point it is also an advantage because of decreasing the melting temperature. The specific heat change for Bi-[*x*] wt.% In (X=12, 15, 35.4, 45, 47.6, 53 and 62) alloys are calculated and presented in Table 1.

In Figure 5, two peaks were observed from the DSC curves of Bi-15 wt.% In ve Bi-47.6 wt.% In alloy systems. When the Bi-In phase diagram is examined for the Bi-15 wt.% In alloy, the melting temperature of Bi_3In intermetallic is observed approximately 382.7 K. It was concluded that the sharp peak in the DSC curve is intermetallic Bi_3In. The curve where the peak temperature arises to 355.171 K was considered as Bi phase. The peak temperature for the Bi-47.6 wt.% In alloy system was analysed as 368.11 K. From the phase diagram, it was observed that there is an intermetallic Bi_3In_5 phase with a melting temperature of 363 K. It was concluded that the curve with the peak temperature of 364.88 K is the γ1 phase which is rich in Bismuth. Although one sharp peak was observed in other alloys, two phases were revealed in the microstructures. Since the phases in the Bi-12wt.% In alloy remain in the same curve and the Bi-[x] wt.% In (X=35.4, 45, 53 and 62) alloys are close to the eutectic point, it is thought that the phases exposed in the microstructure are coincident in the peaks in the DSC curves. Therefore, it is concluded that the coincident phases have the same thermal properties.

Table 1. Some thermodynamic properties of the Bi-In binary alloys as a function of In content.

Composition (wt.%)		Onset Temperature, T_{onset} (K)	Peak Temperature, T_{max} (K)	End Temperature, T_{end} (K)	$\Delta T=T_{end}-T_{onset}$ (K)	Enthalpy of Fusion (J/g)	Specific Heat of Fusion (J/gK)
Bi-12 In		383.84	385.78	386.78	2.94	17.97	0.159
Bi-15 In	Bi	354.43	355.17	355.98	1.55	0.003	$0.364x10^{-4}$
	Bi_3In	382.47	384.61	385.54	3.07	25.14	0.225
Bi-35.4 In		384.27	387.24	388.23	3.96	42.37	0.371
Bi-45 In		366.18	368.27	370.84	4.66	35.36	0.372
Bi-47.6 In	γ1	363.38	364.88	365.62	2.24	0.40	0.004
	Bi_3In_5	365.62	368.11	369.03	3.41	31.79	0.334
Bi-53 In		362.30	367.09	368.08	5.78	29.26	0.311
Bi-62 In		347.01	349.03	353.53	6.52	24.71	0.325

Electrical Conductivity-Temperature Relation

Electrical conductivity-temperature graphs are given in Figure 6. As seen in the graphs electrical conductivities of the systems decrease linearly with increasing temperature.

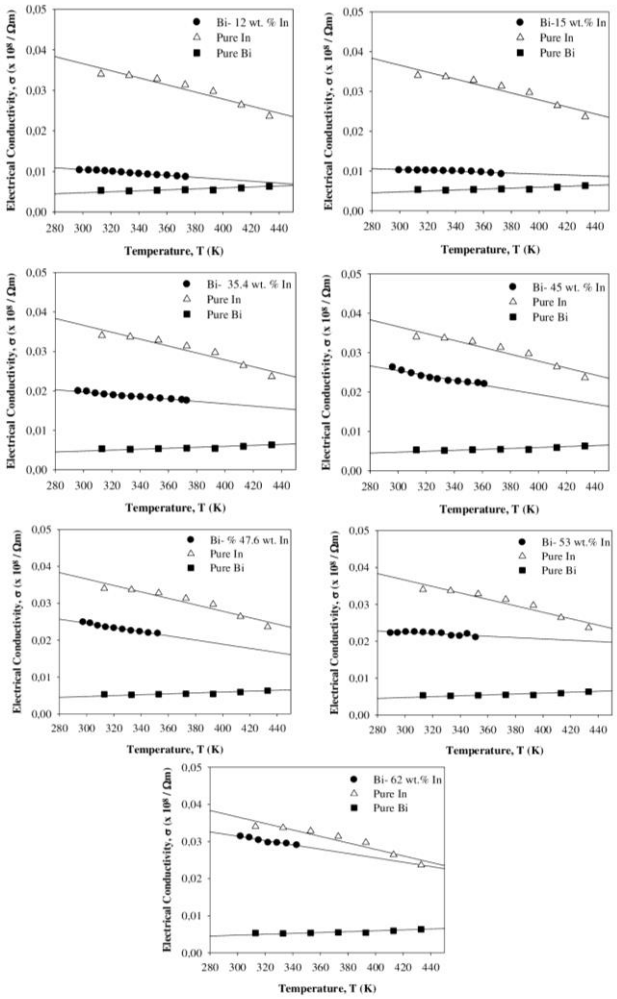

Figure 6. The temperature dependency of electrical conductivity for Bi-In intermetallic alloys.

For Bi-12 wt.% In, Bi-15 wt.% In, Bi-35.4 wt.% In, Bi-45 wt.% In, Bi-47.6 wt.% In, Bi-53 wt.% In and Bi-62 wt.% In alloys, at their melting temperatures, the electrical conductivity values were obtained as 0.8524, 0.9128, 1.6567, 2.1422, 2.0622, 2.1146 and 2.8381 $(\times 10^6)/\Omega$ m, respectively.

In Figure 6, calculated electrical conductivity values were compared to the values of pure Bi and pure In. The electrical conductivity lines for Bi-In intermetallic alloys are between pure Bi and pure In lines. Since Bismuth is semimetal, its electrical conductivity value is about 30 times smaller than Indium's. Therefore, the electrical conductivities of Bi-In intermetallic alloys change with the Bismuth addition in the alloy. As can be seen from the phase diagram and the images of microstructures given in Figure 5, while the amount of Indium in the alloy increases, phase numbers and volume fraction of intermediate phases between Bi and In increase. Therefore, the electrical conductivity of Bi-In alloy increases with increasing the amount of In content in Bi-In alloys and the electrical conductivity lines for Bi-In intermetallic alloys approach to the line of pure Indium.

From electrical conductivity-temperature graphs, electrical conductivity's temperature coefficients were obtained as 2.41, 1.61, 1.95, 2.28, 2.54, 0.46 and 1.65 $(\times 10^{-3})$ K^{-1} respectively (Table 2).

Thermal Conductivity-Temperature Relation

Pure metals have high thermal conductivities, and generally it has been supposed that metal alloys should also have high conductivities. Thermal conductivity of the binary alloy can be expected to lie between the thermal conductivity of its components. However, this turns out not to be the case. The thermal conductivity of binary alloy is usually much lower than that of either metals. Even small amounts in a pure metal of "foreign" molecules that are good conductors themselves seriously disrupt the flow of heat in that metal.

Table 2. Some electrical and thermal properties of solid phase for In-Bi intermetallic alloys.

Materials	Melting Temperature K, (^{0}C)	Temperature Coefficient of Electrical Conductivi α (K^{-1}) x10^{-3}	Temperature Coefficient of Thermal Conductivity α (K^{-1}) x10^{-3}	Electrical Conductivity at the Melting Temperature σ (1/Ω m) ×10^6	Thermal Conductivity at the Melting Temperature K (W/Km)
Bi-12 wt.%In	385.78 (112.78)	2.41	1.36	0.8524	14.50
Bi-15 wt.%In	384.61(111.61)	1.61	1.29	0.9128	16.23
Bi-35.4 wt.%In	387.24 (114.24)	1.95	3.27	1.6567	19.42
Bi-45 wt.%In	368.27 (95.27)	2.28	2.86	2.1422	25.63
Bi-47.6 wt.%In	368.11(95.11)	2.54	2.47	2.0622	25.98
Bi-53 wt.%In	367.06 (94.06)	0.46	1.79	2.1146	31.83
Bi-62 wt.%In	349.03 (76.03)	1.65	4.34	2.8381	35.93

Thermal conductivity-temperature graphs were shown in Figure 4 and the related data are given in Table 3. In Figure 4, a linearly decrease in the values of thermal conductivity is seen with increasing temperature at high temperatures [T >>Debye temperature (Q_D)]. The number of phonons is proportional to the temperature. So the higher the temperature, the more will be the phonon collusion frequency, resulting in smaller mean free paths. Since C_V approaches the constant Dulong-Petit value, the change in the thermal conductivity has overwhelmingly controlled by the variance in mean free path. So that with increasing temperature, thermal conductivity decreases (Touloukian et al., 1970).

Table 3. The experimental data in the measurement of thermal conductivity variations with temperature for Bi-In intermetallic alloys

Bi-12 wt.%In				
T (K)	T(°C)	Q (W)	ΔT (K)	K(W/Km)
313	40	1.41	5.01	16.84
333	60	2.02	7.64	15.76
353	80	2.69	10.24	15.70
373	100	3.37	13.06	15.41

Bi-15 wt.%In				
T (K)	T(°C)	Q (W)	ΔT (K)	K(W/Km)
313	40	1.71	5.63	18.18
333	60	2.66	9.02	17.62
353	80	3.72	12.82	17.31
373	100	4.72	16.99	16.58

Bi-35.4 wt.%In				
T (K)	T(°C)	Q (W)	ΔT (K)	K(W/Km)
313	40	1.15	2.57	26.75
333	60	1.48	3.89	22.73
353	80	1.86	5.12	21.67
373	100	1.96	5.57	20.97

Bi-45 wt.%In				
T (K)	T(°C)	Q (W)	ΔT (K)	K(W/Km)
313	40	1.85	3.63	30.44
333	60	2.74	5.60	29.24
353	80	3.57	7.57	28.16
363	90	4.09	9.57	25.49

Bi-47.6 wt.%In				
T (K)	T(°C)	Q (W)	ΔT (K)	K(W/Km)
313	40	1.58	3.13	30.12
333	60	2.07	4.38	28.27
353	80	2.41	5.30	27.20

Bi-53 wt.%In				
T (K)	T(°C)	Q (W)	ΔT (K)	K(W/Km)
313	40	2.84	4.77	35.57
333	60	3.78	6.57	34.34
353	80	4.31	7.83	32.91

Bi-62 wt.%In				
T (K)	T(°C)	Q (W)	ΔT (K)	K(W/Km)
313	40	2.65	3.69	42.88
333	60	3.69	5.58	39.52
343	70	4.75	7.66	37.04

T: Temperature, **Q:** Heat flow rate into specimen, **ΔT:** Temperature difference into specimen, **K:** Thermal conductivity of specimen.

The melting temperature is the transformation temperature from solid state to liquid state. Thus, thermal properties of materials such as specific heat, thermal conductivity and enthalpy change with the melting temperatures. These kinds of thermal properties play critical role in transformation from liquid to solid or vice versa progress. One of them is the thermal conductivity of materials at its melting temperature. Solidification rate or solid phase growth rate exactly depends on conduction heat transfer rate and their thermal conductivity values and conduction can take place through either solid or liquid depending on the temperature gradients and thermal conductivity of phases at the interface and their thermal conductivities at the melting temperatures, respectively. Consider for example solid growing at a velocity *v* with a planar interface into a superheated liquid. The heat flow away from the interface through the solid must balance that from the liquid plus the latent heat generated at the interface. The value of thermal conductivity at the melting temperature is a required parameter for all kinds of materials. Therefore, the values of K at their melting temperature for Bi-12 wt.% In, Bi-15 wt.% In, Bi-35.4 wt.% In, Bi-45 wt.% In, Bi-47.6 wt.% In, Bi-53 wt.% In and Bi-62 wt.% In alloys were obtained as 14.50, 16.23, 19.42, 25.63, 25.63, 31.83 and 35.93 W/Km, respectively as seen from Table 2.

Also the temperature coefficients of thermal conductivity for same alloy systems were calculated as 1.36, 1.29, 3.27, 2.86, 2.47, 1.79 and 4.34 ($\times 10^{-3}$) K^{-1}, respectively. Electrical temperature coefficient (α_{ETC}) and thermal temperature coefficient (α_{TTC}) are main physical properties of materials. Variations of electrical and thermal conductivities with temperature for solid materials depend on the values of α_{ETC} and α_{TTC}. The values of α_{ETC} and α_{TTC} are usually the highest and the smallest values for good conductor and insulator materials, respectively. As can be seen from Table 2 and Figure 4, it is concluded that the values of α_{ETC} and α_{TTC} increase with increasing In content in the Bi-In alloys.

A comparison was done to obtained and pure Bi, In thermal conductivity values (Figure 4). The thermal conductivity lines for Bi-In intermetallic alloys were occurred between pure Bi and In that shown in Figure 4. As the amount of Indium in the alloy systems increases, the measured thermal conductivity values are close to the thermal conductivity lines of pure Indium. It's seen in Figure 4 that the measured thermal conductivity data are in good compatibility with the thermal conductivity values of pure alloying elements.

Thermal Conductivity's Electron and Phonon Components

As explained above, a LHF system was used to measure the thermal conductivity and a FPP system was used to measure the electrical conductivity values of the binary alloy systems. K_e value was calculated by using the measured σ from Eq. (3) at given temperature. Than K_{ph} was calculated by using the measured $K_{thermal}$ and calculated K_e from Eq. (2). The data that were used is given in Table 4. Also in Figure 7 the electron and phonon contribution to the thermal conductivity versus temperature is given. In Table 4 and Figure 7, it is clearly seen that the value K_e wasn't changed with temperature and stayed constant. Thus it can be said that the results convenient with the WFL. According to this, the K_e is proportional to the product of electrical conductivity with temperature. Because of electrical conductivity decreases with increasing temperature K_e stays constant according to the WFL. Also in Figure 4

and Figure 7 it is seen that $K_{thermal}$ and K_{ph} values linearly decrease with increasing temperature. The percentages of K_{ph} were found as 49-54 %, 49-57 %, 37-52 %, 23-39 %, 30-40 %, 49-52 %, 35-46 % for Bi-12 wt.% In, Bi-15 wt.% In, Bi-35.4 wt.% In, Bi-45 wt.% In, Bi-47.6 wt.% In, Bi-53 wt.% In and Bi-62 wt.% In alloys at between 313-373 K temperature, respectively.

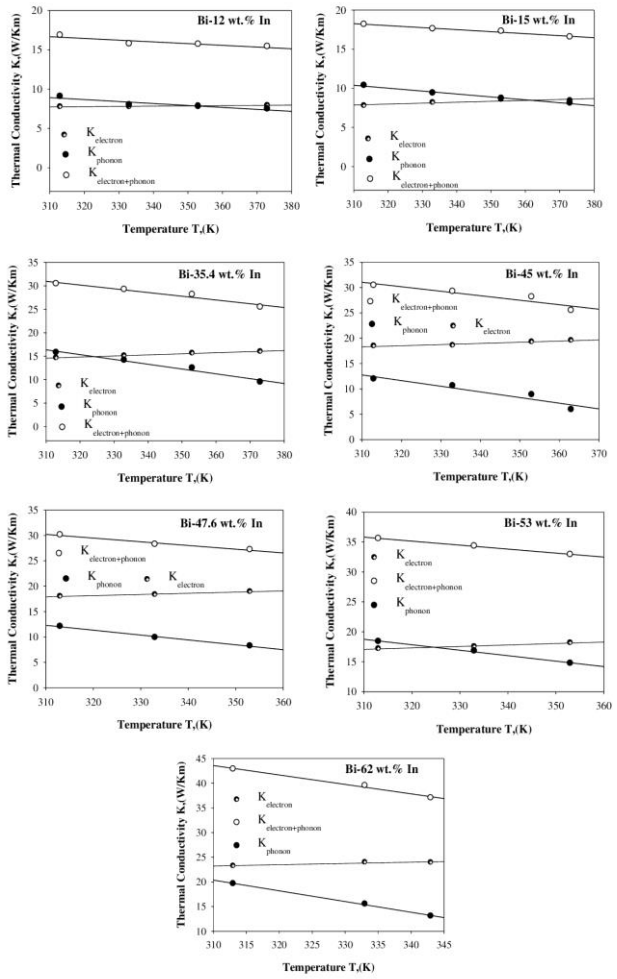

Figure 7. The temperature dependency of the phonon and electron contribution to the thermal conductivity for Bi-In intermetallic alloys.

CONCLUSIONS

The results that were obtained from the study summarized below;

(1) The microstructure of Bi-In intermetallic alloy systems was observed through SEM images and all phases on the samples were determined by EDX analyses. As shown in Figure 4, Bi, Bi_4In, Bi_3In, BiIn, Bi_2In_3, Bi_3In_5, $BiIn_2$ and $BiIn_3$ phases have been detected. The phases obtained on the samples are compatible with the phases on the phase diagram reported in ASM (1992).

Table 4. The temperature dependency of the electron and phonon components to the thermal conductivity for Bi-In intermetallic alloys.

Bi-12 wt.%In				
T (K)	T (°C)	K_e (W/Km)	K_p (W/Km)	$K_{thermal}$ (W/Km)
313	40	7.77	9.07	16.84
333	60	7.75	8.01	15.76
353	80	7.90	7.80	15.70
373	100	7.93	7.48	15.41

Bi-15 wt.%In				
T (K)	T (°C)	K_e (W/Km)	K_p (W/Km)	$K_{thermal}$ (W/Km)
313	40	7.80	18.18	18.18
333	60	8.20	17.62	17.62
353	80	8.58	17.31	17.31
373	100	8.45	16.58	16.58

Bi-35.4 wt.%In				
T (K)	T (°C)	K_e (W/Km)	K_p (W/Km)	$K_{thermal}$ (W/Km)
313	40	14.65	15.79	26.74
333	60	15.09	14.14	22.73
353	80	15.65	12.50	21.67
373	100	15.99	9.50	20.97

Bi-45 wt.%In				
T (K)	T (°C)	K_e (W/Km)	K_p (W/Km)	$K_{thermal}$ (W/Km)
313	40	18.48	11.96	30.44
333	60	18.60	10.64	29.24
353	80	19.29	8.87	28.16
363	90	20.10	5.92	25.49

Bi-47.6 wt.%In				
T (K)	T (°C)	K_e (W/Km)	K_p (W/Km)	$K_{thermal}$ (W/Km)
313	40	18.02	12.10	30.12
333	60	18.36	9.91	28.27
353	80	18.94	8.26	27.20

Bi-53 wt.%In				
T (K)	T (°C)	K_e (W/Km)	K_p (W/Km)	$K_{thermal}$ (W/Km)
313	40	17.18	18.40	35.57
333	60	17.54	16.80	34.34
353	80	18.16	14.74	32.91

Bi-62 wt.%In				
T (K)	T (°C)	K_e (W/Km)	K_p (W/Km)	$K_{thermal}$ (W/Km)
313	40	23.24	19.64	42.88
333	60	23.99	15.53	39.52
343	70	24.65	13.09	37.04

(2) The melting temperatures, the enthalpy of fusion and the specific heat change of Bi-In alloy systems were determined by using DSC measurements. As seen from the results, the measured melting temperatures are in good agreement with the values in Ref ASM (1992).

(3) For the studied systems, it was seen that electrical conductivity and thermal conductivity decrease linearly with increasing temperature between the values of 0.8524 and 2.8381 ($\times 10^6$)/Ωm and 14.50 and 35.93 W/Km, respectively. In addition, it mightily related with the composition of the elements in the system. As the amount of indium increases, the thermal conductivity value increases too.

(4) K_e and K_{ph} values for the systems were obtained with the measured $K_{thermal}$ and σ values by using WFL. It is clearly seen that the K_e values seem to be constant while the values of K_{ph} decrease linearly with increasing temperature. In other words, since the electron mean free path is longer in pure materials, K_e value is dominant at all temperatures. However, in impure materials, K_{ph} approaches to the K_e because of the reducing of the mean free path by collisions with impurities.

AUTHOR CONTRIBUTIONS

P. Ata Esener wrote the manuscript with contributions from Ü. Bayram, E. Öztürk and N. Maraşlı, P. Ata Esener, Ü. Bayram, E. Öztürk and S. Aksöz were

responsible for experimental and analysis periods. S. Aksöz supervised the work and contributed to the writing of the manuscript.

DECLARATION OF COMPETING INTEREST

The authors declare no conflict of interest.

ACKNOWLEDGMENT

Erciyes University Scientific Research Project Unit and Nevşehir Hacı Bektaş Veli University Research Foundation were provided the funding of this study under Contract No: FBA–2013–4746 and NEÜADP15S18, respectively. The researchers thank to the universities for their supports.

REFERENCES

Akbulut S., Ocak Y., Maraşlı N., Keşlioğlu K., Böyük U., Çadırlı E., Kaya H., 2008, Interfacial Energy of Solid In_2Bi Intermetallic Phase in Equilibrium with In-Bi Eutectic Liquid at 72 Degrees C Equilibrating Temperature, *Mat. Charact.*, 59, 1101-1110.

Akbulut S., Ocak Y., Keşlioğlu K., Maraşlı N., 2009, Thermal Conductivities of Solid and Liquid Phases for Neopentylglycol Aminomethylprppanediol and their Binary Alloy, *J. Phys. and Chem. of Solids,* 70, 72-78.

Aksöz N., 2013, *The Determination of Thermophysical Properties of Metallic Alloys*, Nevşehir University Graduate School of Natural and Applied Sciences, M. Sc. Thesis, Nevşehir.

Altıntas Y., Kaygısız Y., Öztürk E., Aksöz S., Keşlioğlu K. and Maraşlı N., 2016, The Measurements of Electrical and Thermal Conductivity Variations with Temperature and Phonon Component of the Thermal Conductivity in Sn–Cd–Sb, Sn–In–Cu, Sn–Ag–Bi and Sn–Bi–Zn alloys, *Int. J. Thermal Sci.*, 100, 1-9.

ASM International Alloy Phase Diagram and the Handbook Committees, 1992, ASM Handbook vol. 3 Alloy Phase Diagrams, 100.

Ata Esener P., Altıntas Y., Bayram Ü., Öztürk E., Maraşlı N., Aksöz S., 2019, Effect of Sn Contents on Thermodynamic, Microstructure and Mechanical Properties in the Zn_{90}–Bi_{10} and Bi_{88}–Zn_{12} Based Ternary Alloys, *J Mater Sci: Mater in Elect.*, 30, 3678-3691.

Bencze P.L., 2006, Mass Spectrometric Determination of Ternary Interaction Parameters of Liquid Cu–In–Sn Alloy, *Int. J. Mass Spectrom.*, 257, 41–49.

Callendar H.L., Nicolson J.T., 1897, Experiments on the Condensation of Steam. Part I. a New Apparatus for Studying the Rate of Condensation of Steam on a Metal Surface at Different Temperatures and Pressures, *Brt. Assoc. Adv. Sci., Rept. Ann. Meeting*, 22, 418.

Gündüz M., Hunt J.D., 1985, The Measurement of Solid−Liquid Surface Energies in the Al−Cu, Al− Si and Pb−Sn Systems, *Acta Metall.*, 33,1651–1672.

Jiang N., Wachsman E.D., Jung S.H., 2002, A Higher Conductivity Bi_2O_3-Based Electrolyte, *Solid State Ionics*, 150, 347–353.

Karadağ S.B., Öztürk E., Aksöz S., Maraşlı N., 2018, Thermophysical Properties of NPG Solid Solution in the NPG-SCN Organic System, *Int. J Mater Res.*, 109, 219-224.

Keşlioğlu K., Böyük U., Erol M., Maraşlı N., 2006, Experimental Determination of Solid-Liquid Interfacial Energy for Succinonitrile Solid Solution in Equilibrium with the Succinonitrile-(D) Camphor Eutectic Liquid, *J. Mat. Sci.*, 41, 7939-7943.

Kittel C., 1965, Introduction to Solid State Physics sixth ed. John Wiley and Sons.

Liu H.Y., Avrutin V., Izyumskaya N., Ozgur U., Morkoc H., 2010, Transparent Conducting Oxides for Electrode Applications in Light Emitting and Absorbing Devices, *Superlat. Microstruct*, 48, 458–484.

Maraşlı N., Hunt J.D.,1996, Solid−Liquid Surface Energies in the Al−$CuAl_2$, Al−$NiAl_3$ and Al− Ti Systems, *Acta Metall.*, 44, 1085–1096.

Meydaneri F., Saatçi B., Ari M., 2012, Thermo-Electrical Characterization of Lead-Cadmium (Pb-Cd) Alloys, *Int. J. Phys. Sci.*, 7 (48), 6210-6221.

Ocak Y., Akbulut S., Keşlioğlu K., Maraşlı N., 2008, Solid-Liquid Interfacial Energy of Aminomethylpropanediol, *J. Phys. D: Appl. Phys.*, 41, 065309.

Onaran K., Material Science, 2009, Science Technique Publisher, İstanbul/Turkey.

Pietenpol W.B., Miley H. A, 1929, Electrical Resistivities and Temperature Coefficients of Lead, Tin, Zinc and Bismuth in the Solid and Liquid States, *Phys. Rev*, 34, 1599.

Rudnev V., Loveless D., Cook R., Black M., 2003, Handbook of Induction Heating. Markel Dekker Inc, New York, 119-120.

Sammes N.M., Tompsett G.A., Nafe H., Aldinger F., 1999, Bismuth Based Oxide Electrolytes Structure and Ionic Conductivity, *J. Eur. Cer. Soc.*, 19, 1801–1826.

Sun H.T., Zhou J., Qiu J., 2014, Recent Advances in Bismuth Activated Photonic Materials, Prog. In Mater. Sci., 64, 1–72.

Tahar R.B.H., Ban T., Ohya Y., Takahashi Y., 1998, Tin Doped Indium Oxide Thin Films Electrical Properties, *J. Appl. Phys.*, 83, 2631–2645.

Takahashi T., Iwahara H., Esaka T., 1977, High Oxide Ion Conduction in Sintered Oxide of the System Bi_2O_3–M_2O_3, *J. Elec. Soc.*, 124, 1563–1569.

Touloukian Y.S., Powell R.W., Ho C.Y., Klemens P.G., 1970, Thermal Conductivity Metallic Elements and Alloys, New York-Washington, vol. 1, 17a.

Touloukian Y.S., Powell R.W., Ho C.Y, Klemens P.G.,1970, Thermal Conductivity Metallic Elements and Alloys, New York, Washington, vol.1, 39-40.

Touloukian Y.S., Powell R.W., Ho C.Y, Klemens P.G.,1970, Thermal Conductivity Metallic Elements and Alloys, *Thermophysical Properties of Matter*, New York - Washington, 13a-25a, 49, 149, 185, 408, 498, 845.

Valder L.B., 1954, Resistivity Measurements on Germanium for Transistors, *Proc. IRE*., 42, 420-427.

Vizdal J., Braga M.H., Kroupa A., Richter K.W., Soares D., Malheiros L.F., Ferreira J., 2007, Thermodynamic Assessment of the Bi–Sn–Zn System, *Calphad*, 31, 438–448.

Yang W., Messler Jr R.W., 1994, Microstructure Evolution of Eutectic Sn-Ag Solder Joints, *J. Electron. Mater.*, 23(8), 765-772.

Yang S.B., Kong B.S., Jung D.H., Baek Y.K., Han C.S., Oh S.K., Jung H.T., 2011, Recent Advances in Hybrids of Carbon Nanotube Network Films and Nanomaterials for their Potential Applications as Transparent Conducting Films, *Nanoscale* 3, 1361–1373.

Yılmaz S., 2008, *Synthesis, Characterization and Investigation of the Solid State Oxygen Ionic Conductivities of Beta-Bi2o3 Type Solid Electrolytes Doped with Dy2o3, Eu2o3, Sm2o3*, Gazi University, Institute of Science and Technology, Ph.D. Thesis, Ankara.

Pınar ATA ESENER graduated from Physics Department of Nevşehir Hacı Bektaş Veli University in 2012. She received his MSc degree from Physics Department of Nevşehir Hacı Bektaş Veli University in 2015. She received his second MSc degree from Metallurgical and Materials Engineering Department of Nevşehir Hacı Bektaş Veli University (Erciyes University joint program) in 2015. She is currently doing her doctorate in the Department of Materials Science and Engineering (YÖK 100/2000 Micro and Nanotechnology) at Erciyes University.

Ümit BAYRAM graduated from the Physics Department of Cumhuriyet University in 2008. Then, in 2011, he completed his master's degree in Erciyes University Physics Department and started to work as a Research Assistant in the same year. He completed his PhD in 2017 by taking part in different scientific projects in the field of Solid State Physics. Currently, Erciyes University continues his doctorate education in the field of Nanoscience and Nanotechnology for the second time. His fields of study include Nanotechnology, Materials Science, Environment and Ecology, Production and Characterization of Nanomaterials, Spectroscopy and Water Resources.

Esra ÖZTÜRK graduated from Physics Department of Kocaeli University in 2005 (Kocaeli, Turkey). She received her MSc degree from both Kocaeli University Physics Department and Paris 13 University Galilee Institute (L.P.M.T.M.) in 2008 (Paris, France). She received her PdD degree from Erciyes University in 2016 (Kayseri, Turkey). She has been working as a Research Assistant in Kocaeli University since 2010. Her research interests are Solid-Liquid Interfacial Energy of Metallic Alloy Systems, Lead-Free Solder Systems, Solidification, Phase Transitions, Thin Film's Optical and Magnetic Properties.

Sezen AKSÖZ graduated from Physics Department of Erciyes University in 2003 (Kayseri, Turkey). She received her MSc and PhD degree from Erciyes University Physics Department in 2006 and in 2010, respectively. She worked as an Assistant Professor between 2010-2012 and Associate Professor between 2012-2017 in Nevşehir Hacı Bektaş Veli University. She has been working as a Professor since 2017 in the same university. Her research interests are Solid-Liquid Interfacial Energy of Metallic Alloy Systems, Lead-Free Solder Systems, Organic Compounds, Solidification, Phase Transitions.

Necmettin MARAŞLI received his Ph.D. degree from Oxford University, Department of Materials, England in 1995. He is a full professor at Department of Metallurgical and Materials Engineering, Yıldız Technical University İstanbul-Turkey. His research interests include directional solidification, solid-liquid interfacial energy measurements, variation of thermal and electrical conductivities with temperature measurements and dependence of mechanical and thermophysical properties on growth rates in the multicomponent metallic and transparent organic alloys. Recently he is studying on solidifications of alloy under uniform static high electrical fields. He has led 45 research projects and 130 scientific papers published in SCI and SCI-expanded indexed Journals, have high impact factor. He also serves as editorial board and reviewer for many international journals.